

## Further-inspection for Doubly-Fed Converter: Theory, Method and Experimental Platform

Zhuo Chen<sup>1</sup>, Zhengping Zhang<sup>2\*</sup>, Zhenghang Hao<sup>3</sup>, Shaohua Li<sup>3</sup>  
and Ailing Zhang<sup>3</sup>

<sup>1</sup>*Department of Electrical Engineering, Guizhou University  
Guiyang, 550025, China*

<sup>2</sup>*College of Computer Science & Technology, Guizhou University  
Guiyang, 550025, China*

<sup>3</sup>*XJ Electric CO., LTD Xuchang, 461000, China*

<sup>1</sup>*ee.chenz@gzu.edu.cn*, <sup>2</sup>*zhengping\_zhang@126.com*, <sup>3</sup>*haozhenghang@163.com*

### Abstract

*In recent years, the interest in the use of regenerative energies has increased considerably, which helped to alleviate the energy crisis and to protect the environment. However, the over-rapid development of wind power also leads to some problems in China, for example, several large-scale off-grid accidents caused by quality problems of wind turbines. Since converter is a core component of wind power turbine, improving converter control strategy can prevent such accidents. Therefore, this paper explores and analyzes the converter control strategy and its influences on power grid and wind turbines, including grid power and voltage fluctuation, small signal stability, transient stability, LVRT (low voltage ride through), shaft damping, and shaft transient stress. This paper attempts to determine the content and method for quality inspection of converter and proposes a test platform to carry out flexible, efficient and reliable quality test.*

**Keywords:** DFIG, rotor-side converter, converter quality inspection, test platform

### 1. Introduction

In the last decades, the international community has been attaching great importance to wind power as a substitute for fossil-fuel energy. In recent years, the development of wind power is speeding up in many countries. In early 2013, installed capacity of the wind turbine generators reached 75 gigawatts in China, surpassing the United States to become the world's largest wind-power producer [1]. However, several large-scale off-grid accidents raised people's awareness of the importance of operational safety [2]. According to some experts in the field, problems brought by the explosive development of wind power began to emerge. Therefore, it is high time that people tackled these problems to ensure the healthy growth of wind-power industry [3]. Many published papers have proved that targeted optimizing the control strategies can reduce the possibilities of such accidents [4-12]. The published literatures [13-15] pointed out overload capacity of rotor-side converter and control strategy for rotor current are bottlenecks in solving the low voltage tolerance problem of DFIG (doubly fed induction generator). The proposed method designed the control parameters for rotor-side converter of DFIG to resist against voltage fluctuation in power grids. The

---

\* Corresponding Author

literature [16] presented an additional damping control method for the original double closed-loop structure, which greatly improves the damping of power system. The literature [17] put forward the double-current control strategy on DC side according to the operational features of the power grid failure, which ensures an excellent dynamic regulation performance even when power grid has asymmetric failure or frequency fluctuations. According to the fact that the converter is possible to be damaged by the over-current of the rotor during the grid voltage recovering period, the literature [18] optimized the current control strategy to restrain the rotor current.

It is thus clear that optimization of control strategy is a solution to wind power accidents. It is also undeniable that poor quality is one of the important causes for the accidents. Due to the limited technology and accumulation knowledge, home-made wind generating equipments have poor qualities. The manufacturers of introducing foreign technology are also limited to assembling units based on the design drawings. As these manufacturers lag behind in technology and innovation, the quality of their production needs to be improved [2-3]. Therefore, stepping up quality test technology for the wind power machinery and equipment, especially the critical components, and establishing a test platform are two urgent tasks for wind power development. The converters are the high-technology critical component in the doubly-fed wind turbine system. The performance of the converter determines the reliability, safety, stability and power quality of grid-connected wind power system. The role of the target equipment in the wind power system is needed to explore as well as its interaction with other components before determining the content and the method and the platform for the quality inspection of doubly-fed converter.

This paper analyzes the role of doubly-fed converter in power grid and its interaction with wind turbines by simulation. It also examines the influence of doubly-fed converter on voltage fluctuations, small signal stability, transient stability, LVRT, shaft damping, and shaft transient stress under different control strategies. Finally, this paper proposes a theoretical framework for the test content and method of doubly-fed converter and sets up an effective test platform.

This paper is organized as follows: The second part describes the mathematical model for doubly-fed wind power system, including the turbine model, the power generator model and the vector control strategy. The influence of doubly-fed converter on power grid is discussed in the third part from the following perspectives: power and voltage, small signal stability, transient stability, and LVRT. The fourth part explores the influence of doubly-fed converter on turbines from shaft damping and shaft transient stress. The fifth part proposes a test platform and the test content for quality inspection of the wind power equipments. Finally, the sixth part summarizes the theoretical basis, test content and test platform for converter quality inspection.

## **2. Modelling of Doubly-fed Wind Power System**

### **2.1 Structure of doubly-fed wind power system**

Figure 1 shows the schematic diagram of wind turbine with DFIG connected to an infinite bus through the transformer. The stator of DFIG is directly connected to the power grid, and the rotor windings are supplied from the double fed converter via slip rings. The double fed converter consists of two back-to-back voltage source converters (VSCs), which are close to the rotor side (machine-side converter) and the grid side (grid-side converter). The machine-side converter is a critical component of doubly-fed wind power system because it provides the ac excitation current for the rotor of doubly-

fed asynchronous generator and because it supplies the power flow path from the rotor to the grid. Therefore, it is also a critical test content for the quality of doubly-fed power system.

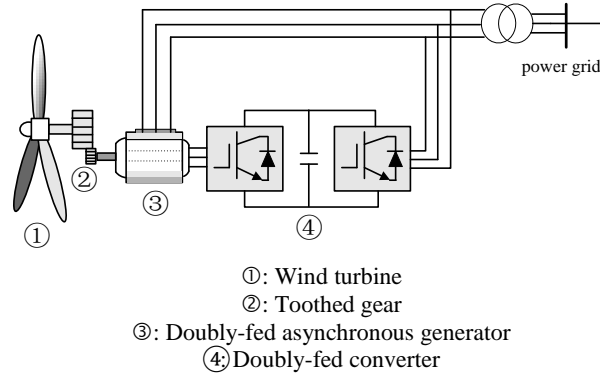


**Figure 1. Structure of Doubly-fed Wind Power System**

## 2.2 Turbine Model

Based on the steady-state power characteristics of the turbine, the mechanical power captured by the turbine from the wind is given by the following equation [19]:

$$P_m = \frac{\rho A}{2} C_p(\lambda, \beta) v_{wind}^3$$

Where  $P_m$  is the mechanical output power of the turbine (W),  $\rho$  is the air density ( $\text{kg/m}^3$ ),  $A$  is the turbine swept area ( $\text{m}^2$ ),  $C_p(\lambda, \beta)$  is the performance coefficient of the turbine,  $\lambda$  is the tip speed ratio of the rotor blade tip speed to wind speed,  $\beta$  is the blade pitch angle (deg) and  $v_{wind}$  is the wind speed (m/s).

## 2.3 Modelling of the DFIG

The stator flux linkage ( $\psi_{ds}, \psi_{qs}$ ) and the rotor circuit ( $i_{dr}, i_{qr}$ ) are chosen as the state variables in d-q reference frame with the stator voltage orientation. The following equations are used to model the DFIG generator [20]:

$$p\psi_{ds} = -\frac{r_s}{l_s}\psi_{ds} + l''r_s i_{dr} + \omega_1\psi_{qs}$$

$$p\psi_{qs} = -\frac{r_s}{l_s}\psi_{qs} + l''r_s i_{qr} - \omega_1\psi_{ds} + u_{qs}$$

$$pl'i_{dr} = -r_r i_{dr} + u_{dr} + \omega_s l' i_{qr} + \omega_s l'' \psi_{qs} - l'' p\psi_{ds}$$

$$pl'i_{qr} = -r_r i_{qr} + u_{qr} - \omega_s l' i_{dr} - \omega_s l'' \psi_{ds} - l'' p\psi_{qs}$$

Where,  $l' = (l_r - \frac{l_m^2}{l_s})$ ,  $l'' = \frac{l_m}{l_s}$ ,  $l_s$  and  $l_r$  are the stator and rotor self-inductances,  $l_m$  is the mutual inductance,  $r_s$  and  $r_r$  are the stator and rotor resistances,  $\omega_1$  and  $\omega_s$  are the

synchronous speed and the slip speed,  $u_{dr}$  and  $u_{qr}$  are exciting voltages,  $u_{qs}$  is the stator voltage and  $p$  is the differential operator.

## 2.4 Doubly-fed converter control model

The machine-side converter is connected to the rotor of the power generator. In order to implement the independent control for active power and reactive power, the direction of stator voltage vector is determined the direction of axis d and the vector control is applied to decouple the mechanical sub-system and the electrical sub-system in the wind turbine system. The literature [21] described the control diagram for machine-side converter, as shown in Figure 2.

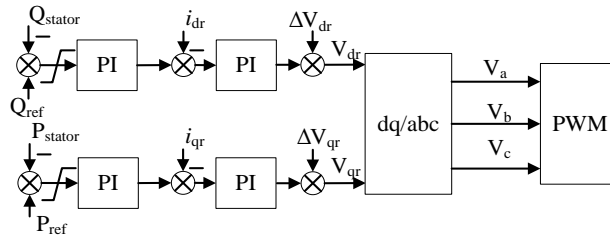


**Figure 2. Control Block Diagram of Rotor-side Converter**

The control system for machine-side converter controls rotor current and voltage in order to output modulation wave and compares the modulation wave with the carrier signal to generate the pulse control signal what can achieve on-off control of power electronic devices, so that the control system can realize the electromechanical decoupling of wind power generator.

As shown in Figure 2, the machine-side converter utilizes the PI control system in the power and current double-closed loop to compare reactive  $Q_{stator}$  and active  $P_{stator}$  received from the stator side with the reactive reference  $Q_{ref}$  and the active reference  $P_{ref}$  respectively.

Axis d reference value and axis q reference value of rotor current are made available through the first PI controller. The output voltages  $V_{dr}$  and  $V_{qr}$  are calculated by comparing these reference values with the feedback currents  $i_{dr}$ ,  $i_{qr}$  and adding voltage compensations  $\Delta V_{dr}$  and  $\Delta V_{qr}$  to the PI controller output.  $V_a, V_b, V_c$  are modulation waves actualizing the on-off control of the main circuit.  $\Delta V_{dr}$  and  $\Delta V_{qr}$  are used to eliminate electromechanical coupling. The expressions for  $\Delta V_{dr}$  and  $\Delta V_{qr}$  are shown below:

$$\Delta V_{dr} = k\omega_s \left[ \left( L_r - \frac{L_m^2}{L_s} \right) i_{qr} + \frac{L_m^2}{L_s} \psi_{qs} \right] \quad (1)$$

$$\Delta V_{qr} = k\omega_s \left[ \left( L_r - \frac{L_m^2}{L_s} \right) i_{dr} + \frac{L_m^2}{L_s} \psi_{ds} \right] \quad (2)$$

Where  $\psi_{ds}$  and  $\psi_{qs}$  are the stator flux linkages of axis d and axis q.  $L_s, L_r$  and  $L_m$  are the stator inductance and the rotor inductance and the mutual inductance respectively.  $\omega_s$  is the slip.  $k$  is the coefficient for compensation depth.  $k=1$  means perfect compensation, and  $0 < k < 1$  means under-compensation and  $k > 1$  means over-compensation.



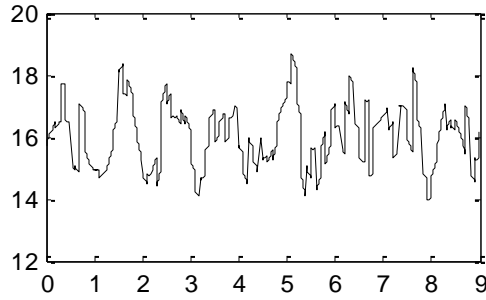


**Figure 4. The Curve of Wind Speed**

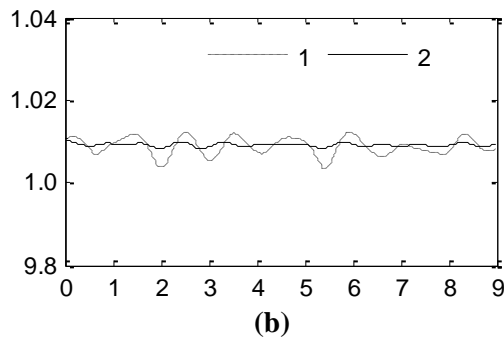
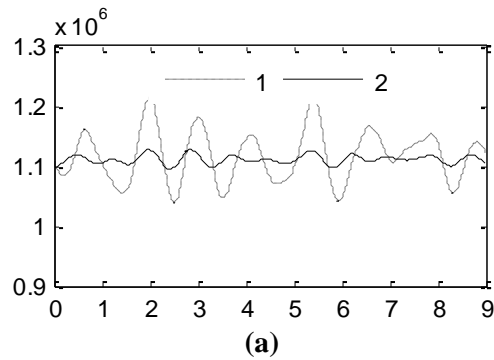


**Figure 5. Influence of Different Control Strategies on Power and Stator Voltage under Different Wind Speed Fluctuations**

Curve 1 and curve 2 represent two control strategies without and with feed-forward compensation respectively.

- (a) Power fluctuation curve
- (b) Voltage fluctuation curve

### 3.2 The influence of machine-side converter on small signal stability

The influence of DFIG on small signal stability of power grid generally depends on the control strategy of excitation converter. The literature [23] presented that the improper excitation control parameters may aggravate the damping of the synchronous generator. This paper uses two control strategies to prove this conclusion. Strategy 1 is the proportional (P)

control of power and current double closed-loop; strategy 2 is the proportional integral (PI) control of power and current double closed-loop. When  $t=0$ , the single line from bus B1 to B2 breaks; when  $t=0.1s$ , the failure is removed. Figure 6 shows the power angle curves of the synchronous generator. It is shown that, compared with strategy 2, strategy 1 produces larger oscillation amplitude and longer oscillation time. Therefore, the PI control of power and current double closed-loop has better performance than the P control.

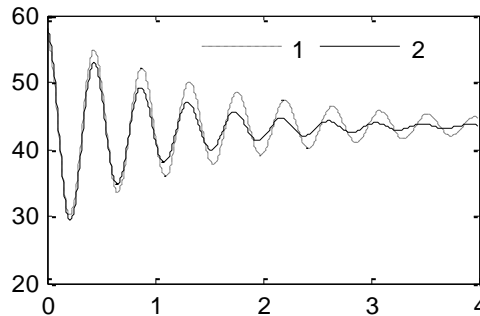


**Figure 6. Influence of different control strategies on power angle of synchronous power generator under small disturbance**

Curve1 represents the proportional (P) control of power and current double closed-loop

Curve2 represents the proportional integral (PI) control of power and current double closed-loop.

### 3.3 The influence of machine-side converter on transient stability

The literature [24] determined the power angle of DFIG and also analyzed the interaction between the synchronous generator and DFIG to explain how DFIG undermines the first-swing stability of the power angle of the synchronous generator when the power system is suffering faults. Since the control characteristics of the machine-side converter can influence the transient active power output and the power angle, the different control strategies also may influence the first-swing stability of the power angle of the synchronous generator. The power loop gain of strategy 1 is set as 0.009 while the power loop gain of strategy 2 is set as 0.002. When  $t=0$ , there is a three-phase short circuit fault between bus B1 and B2; when  $t=0.2s$ , the fault is removed. On this condition, the curves about the power angle oscillation of the synchronous generator under the strategy 1 and strategy 2 are shown in Figure 7. In the beginning, both two curves of power angle reach a certain value and then swing back to the starting value, however, the maximum angle under strategy 2 is  $85^\circ$  and the maximum angle under strategy 1 exceeds  $90^\circ$ . Therefore, different control strategies can lead to different first-swing stability of the synchronous generator.

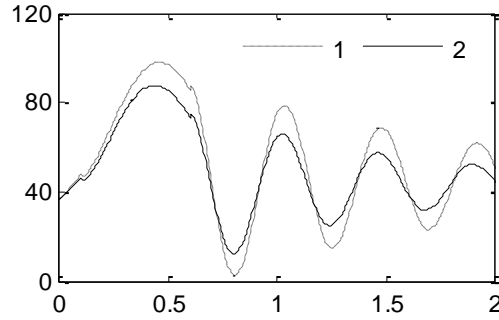


**Figure 7. Influence of Different Control Strategies on First-swing Stabilities of Synchronous Power Generator**

Curve 1: power loop gain is 0.009  
Curve 2: power loop gain is 0.002

### 3.4 The influence of doubly-fed converter on LVRT

The LVRT ability of wind power generator refers to the capacity of restoring the power system voltage by supplying the reactive power to the power grid and avoiding off-grid accident when the grid faults happen. LVRT is an important performance which is used to estimate the reliability of power system with wind power integration. It is also a vital technical condition for wind farm to be connected into the power system. However, there are many factors influencing LVRT, especially the machine-side converter can't be ignored. When  $t=0.8s$ , system voltage decreases by 50% and the fault lasts for 0.5s. Strategy 1 adopts the PI control of the current loop and strategy 2 employs the PI control of the power and current double closed-loop. Figure 8 shows the stator reactive power curves under the two control strategies.

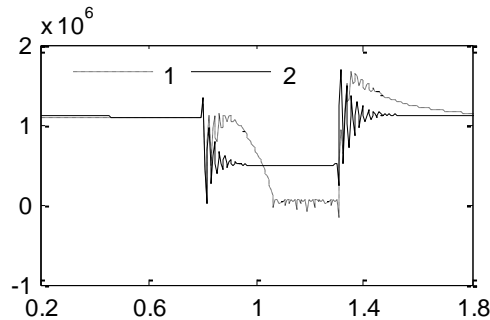


**Figure 8. Stator Reactive Curves of Wind Power Generator under Different Control Strategies**

Curve1: PI control of current loop  
Curve2: PI control of the power and current double closed-loop

As shown in Figure 8, during the grid failure, strategy 2 reduces reactive power by 50% but it can still provide reactive power to the grid. Strategy 1 reduces reactive power to 0var so that it cannot provide enough reactive power to the grid. In addition, when failure is removed, recovery time of reactive power under strategy 1 is longer than under strategy 2.

## 4. The influence of doubly-fed converter on the wind turbine

It was shown in the published paper [25] that because the wind turbine and the wind power generator are connected by the mechanical transmission shaft, the dynamic characteristics of the shaft are likely to be influenced by the electrical subsystem, the geometric construction, material properties and the external airflow. Once the influence is so serious enough that the torsional vibration occurs, the grid safety must be threatened and undermined. As the machine-side converter is a key component in the electrical subsystem, its control strategy will determine the safety of turbine shaft. Therefore, the influence of the machine-side converter on the turbine should be considered and should be included in the test content of the quality inspection in order to provide evidence for the safe operation of the wind power grid-connected.

### 4.1 The influence of the machine-side converter on shaft damping

On the premise of accurate feed-forward compensation, the compensation coefficient  $k$  in equation (1) and (2) is set as 1. On this condition, the electromechanical system can be decoupled entirely. In this way, the shaft damping only depends on the mechanical inherent torsional damping rather than the electrical damping. On the contrary, if feed-forward compensation is not perfect, namely when  $k \neq 1$ , the shaft damping subjects to both the mechanical inherent torsional damping and the electrical damping. Also, it should be paid more attention that electrical subsystem may produce the negative damping torque which is possible to weaken the shaft damping. This section applies two different control strategies to study the influence of different compensation degree on the shaft damping. Strategy 1 represents a 50% feed-forward compensation ( $k=0.5$ ); strategy 2 represents a perfect feed-forward compensation ( $k=1$ ). The wind speed decreases from 15m/s to 9m/s and then increases again to 15m/s. based on the two strategies, the curves of the relative speed between shaft of the wind turbine and rotor of the wind power generator are shown in Figure 9.

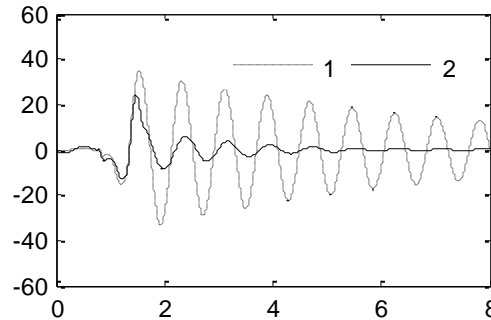


**Figure 9. Relative Speed of Shaft of the Wind Turbine and Rotor of the Wind Power Generator with Different Compensation Depths**

Curve1: 50% feed-forward compensation

Curve2: perfect feed-forward compensation

In Figure 9, the oscillation amplitude of the relative speed with the control strategy 1 is larger and the oscillation time is longer than that with the control strategy 2, because the electromechanical decoupling is inadequate and shaft damping is influenced by electrical damping. Although we can hardly achieve perfect decoupling in most projects, strategy 2 indeed can improve the system damping.

#### 4.2 The influence of the machine-side converter on shaft transient stress

As aforementioned in 4.1, the machine-side converter may reduce the shaft damping and even cause torsional vibration. When rotor is influenced by torque vibration, it will produce a transient stress from the rotor shaft internal to balance the external torque. However, excessive or frequent transient stress can shorten the service life of the rotor and even cause accidents. According to the mechanics theories, external torque is closely related to rotor speed. Therefore, the change of transient stress can be reflected by the change of rotor speed. This section applies two groups of controller parameters which represent two different control strategies to study the influence of the strategies on transient stress of the wind turbine shaft. Strategy 1 is the integral coefficient  $K_i=0.1$  and the proportional coefficient  $K_p=0.02$  in the current loop. Strategy 2 is the integral coefficient  $K_i=0.4$  and the proportional coefficient  $K_p=0.05$  in the current loop. When  $k=0.8$ , the relative speed between the shaft of the wind turbine and the rotor of the wind power generator is calculated and is shown in Figure 10. It's clear that strategy 1 produces larger fluctuations of relative speed than strategy 2, which means its torque stress on the shaft is greater than that of strategy 2.

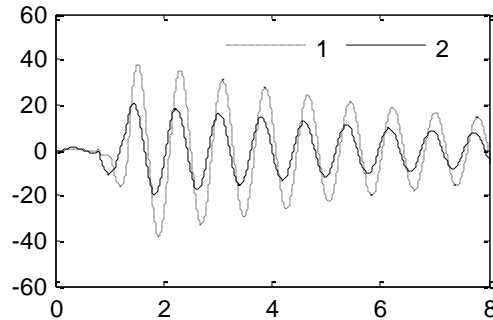


**Figure 10 Relative Speeds between Shaft of the Wind Turbine and Rotor of the Wind Power Generator with Different Controller Parameters**

Curve1: integral coefficient  $K_i=0.1$  and the proportional coefficient  $K_p=0.02$  in the current loop

Curve2: integral coefficient  $K_i=0.4$  and the proportional coefficient  $K_p=0.05$  in the current loop

#### 5. Test Platform Design

According to the analysis mentioned above, a test platform for comprehensive and thorough inspection to the converter is proposed. Figure 11 shows the structure of the test platform.

In the test platform, the power system with wind power consists of four parts, namely the primary side of power grid, the secondary side of power grid, the primary side of the wind power system and the secondary side of the wind power system. The first part of the platform, the primary side of power grid, can be imitated by real time digital simulator (RTDS) which is used to establish a digital simulation platform of the power system. This digital simulation platform can simulate the synchronous generators and the primary side components of the

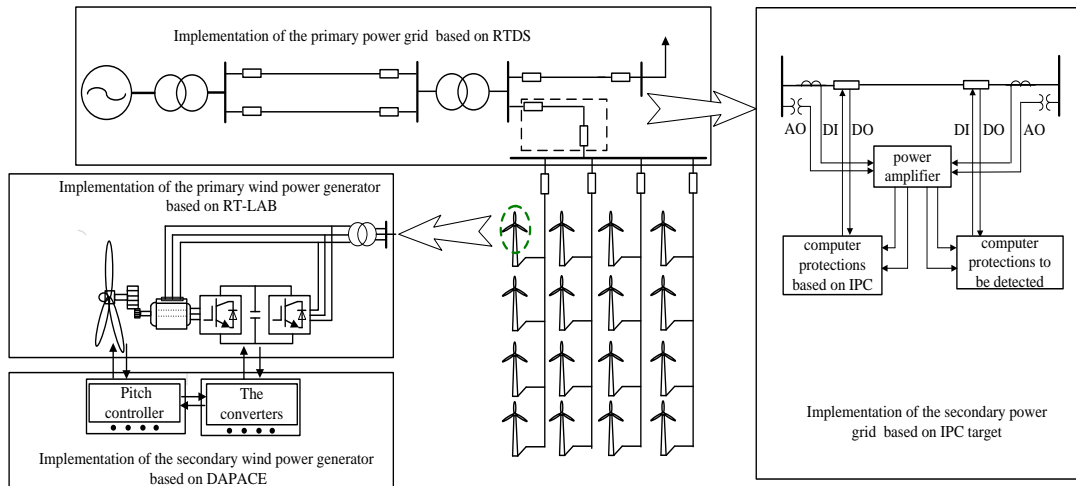


**Figure 11 Design of the Test Platform**

Transmission, and distribution system and various kinds of typical test systems. IPC target is planned to model the secondary side of power grid including the controller and the components of grid protection and communication. Moreover, IPC target even can be linked with the physical equipments to detect their performances. The primary side of wind power system including wind turbine, gear box, wind power generator and converters can be modeled by RT-LAB. The secondary side of wind power is simulated by DSPACE, which not only can design the whole control system in the wind power system, but also can be connected to the physical devices.

In this test platform, the flexible primary side system based on RTDS and RT-LAB, which can be used to build any grid topologies required, overcomes many difficulties in physical modeling. The secondary system based on IPC target and DSPACE supplies various graphical programming languages and an I/O board linking to the control algorithm and the object controlled. The test platform is an effective evaluation system which can explore the influence of the converter on the power grid and the interaction between the wind turbine generator and the power grid.

This test platform can also be used to study the problem associated with other new energies accessing in the smart grid and to provide the quality inspection method and technology for new energy equipments and other equipments connected the power grid.

## 6. Conclusion

In order to provide a theoretical basis for the test contents of quality inspection to the doubly-fed converter, this paper studies the impact of the rotor-side converter on the power grid and the wind turbine. In terms of the influence of the rotor-side converter on the power grid, the control strategy with rotate-speed feed-forward compensation is applied to mitigate the fluctuations of the active power and the generator voltage. Moreover, PI control in the power and current double closed-loop demonstrates better performance than P control under small disturbance. During the three-phase fault period, the excellent parameter, such as the gain in the power loop of the rotor-side converter, is to guarantee the first swing stability of the power angle of synchronous generator. Furthermore, the correct control strategy not only can effectively avoid off-grid accident but also can provide the reactive power to recover the grid voltage.

In terms of the influence of the rotor-side converter on the wind turbine, change of the wind speed can cause the turbine shaft swing and even result in torsional vibration in case electromechanical decoupling is Imperfect. Meanwhile, Change in PI parameters may cause the shaft stress change and then lead to premature fatigue in the shaft. In addition, to carry out in-depth quality inspection for the converter, this paper designs an experimental platform based on advanced simulation techniques, including RTDS, RT-LAB, DSPACE and XPC target. This test platform is a semi-physical platform which not only can replace physical equipment but also can allow the direct connection with the physical devices. It is a high-level and multi-function experimental platform and can be continuously upgraded according to the need. Therefore, the efficient and flexible platform is preferred over the traditional physical test platform.

## Acknowledgements

The authors gratefully acknowledge the support of Social Development Research Project of Guizhou Province, China (SY[2011]3081), and the National Natural Science Fund of China (51267003) and the XJ Electric Co., Ltd, Project.

## References

- [1] Z. Ming, Z. Kun and D. Jun, "Overall review of China's wind power industry: Status quo, existing problems and perspective for future development", *Renewable and Sustainable Energy Reviews*, vol. 3, no. 24, (2013).
- [2] X. Ye, Y. Qiao and Z. Lu, "Cascading tripping out of numerous wind turbines in China: Fault evolution analysis and simulation study", *IEEE Power and Energy Society General Meeting, San Diego, California, USA*, (2012) July 22-26.
- [3] L. Bin, Z. Jingyang, P. Yi, L. Qiang, *et al.*, "Review of Generation Schedule Methods with Large-Scale Wind Power Integration", *Power and Energy Engineering Conference, Wu Han, China*, (2011) March 25-28 .
- [4] D. Campos-Gaona, Member, E. L. Moreno-Goytia and O. Anaya-Lara, "Fault Ride-Through Improvement of DFIG-WT by Integrating a Two-Degrees-of-Freedom Internal Model Control", *IEEE Transactions on Industrial Electronics*, vol. 3, no. 60, (2013).
- [5] M. Rahimi and M. Parniani, "Coordinated Control Approaches for Low-Voltage Ride-Through Enhancement in Wind Turbines With Doubly Fed Induction Generators", *IEEE Transactions on Energy Conversion*, vol. 3, no. 25 (2010)
- [6] M. Boutoubat, L. Mokrani and M. Machmoum, "Control of a wind energy conversion system equipped by a DFIG for active power generation and power quality improvement", *Renewable Energy*, vol. 2, no. 50, (2013)
- [7] J. Martinez, P. C. Kjær, P. Rodriguez and R. Teodorescu, "Design and Analysis of a Slope Voltage Control for a DFIG Wind Power Plant", *IEEE Transactions on Energy Conversion*, vol. 1, no. 27, (2012)
- [8] M. Kayıkci and J. V. Milanovic, "Reactive Power Control Strategies for DFIG-Based Plants", *IEEE Transactions on Energy Conversion*, vol. 2, no. 22, (2007).
- [9] Z. Miao, L. Fan, D. Osborn and S. Yuvarajan, "Control of DFIG-Based Wind Generation to Improve Interarea Oscillation Damping", *IEEE Transactions on Energy Conversion*, vol. 2, no. 24 (2009).
- [10] L. Fan, H. Yin and Z. Miao, "On Active/Reactive Power Modulation of DFIG-Based Wind Generation for Interarea Oscillation Damping", *IEEE Transactions on energy Conversion*, vol. 2, no. 26, (2011)
- [11] K. E. Okedu, S. M. Muyeen, R. T. Hashi and J. Tamura, "Wind Farms Fault Ride Through Using DFIG With New Protection Scheme", *IEEE Transactions on Sustainable Energy*, vol. 2, no. 3 (2012).
- [12] L. Meegahapola, T. Littler and S. Perera, "Capability curve based enhanced reactive power control strategy for stability enhancement and network voltage management", *Electrical Power and Energy Systems*, vol. 5, no. 2, (2013)
- [13] K. E. Okedu, S. M. Muyeen, R. Taka Hashi and J. Tamura, "Wind Farms Fault Ride Through Using DFIG With New Protection Scheme", *IEEE Transactions on Sustainable Energy*, vol. 2, no. 3, (2012).
- [14] H. Geng, C. Liu and G. Yang, "LVRT Capability of DFIG-Based WECS Under Asymmetrical Grid Fault Condition", *IEEE Transactions on Industrial Electronics*, vol. 6, no. 60, (2013)
- [15] Z. Xueguang, P. Weiming, L. Yicheng and X. Dianguo, "Improved grid voltage control strategy for wind farms with dfigs connected to distribution networks", *Journal of Power Electronics*, vol. 3, no. 12, (2012).
- [16] H. Huang and C. Y. Chung, "Coordinated Damping Control Design for DFIG-Based Wind Generation Considering Power Output Variation", *IEEE Transactions on Power Systems*, vol. 4, no. 27, (2012)

- [17] A. H. M. A. Rahim and I. O. Habiballah, "DFIG rotor voltage control for system dynamic performance enhancement", *Electric Power Systems Research*, vol. 2, no. 81, (2011).
- [18] G. Pannell, B. Zahawi, D. J. Atkinson and P. Missailidis, "Evaluation of the Performance of a DC-Link Brake Chopper as a DFIG Low-Voltage Fault-Ride-Through Device", *IEEE Transactions on Energy Conversion*, vol. 3, no. 28, (2013).
- [19] M. Boutoubat, L. Mokrani and M. Machmoum, "Control of a wind energy conversion system equipped by a DFIG for active power generation and power quality improvement", *Renewable Energy*, vol. 2, no. 50, (2013).
- [20] M. Rahimi and M. Parniani, "Transient Performance Improvement of Wind Turbines With Doubly Fed Induction Generators Using Nonlinear Control Strategy", *IEEE Transactions on Energy Conversion*, vol. 2, no. 25, (2010).
- [21] R. K. Behera and S. Behera, "Design, simulation and experimental realization of nonlinear controller for GSC of DFIG system", *World Acad. Sci. Eng. Technol*, vol. 5, no. 6, (2011).
- [22] M. Rahimi and M. Parniani, "Dynamic behavior analysis of doubly-fed induction generator wind turbines – The influence of rotor and speed controller parameters", *International Journal of Electrical Power & Energy Systems*, vol. 5, no. 32, (2010).
- [23] D. Gautam, L. Goel, R. Ayyanar, V. Raja, "Control strategy to mitigate the impact of reduced inertia due to doubly fed induction generators on large power systems", *IEEE Transactions on Power Systems*, vol. 1, no. 26, (2011).
- [24] K. Yun-Seong and W. Dong-Jun, "Mitigation of the flicker level of a DFIG using power factor angle control", *IEEE Transactions on Power Delivery*, vol. 4, no. 24, (2009).
- [25] M. Endusa, B. Senjyu T. Uehara A. Funabashi, *et al.*, "LQG design for megawatt-class WECS with DFIG based on functional models' fidelity prerequisites", *IEEE Transactions on Energy Conversion*, vol. 4, no. 24, (2009).

## [APPENDIX]

The generators' parameters:

Rated stator voltage: 0.69 kV; Rated ro-tor voltage: 1863 V; Rated apparent power: 1667 kVA;

Rated speed: 1800 rpm; No. pole pairs: 2; Stator resistance: 0.008 $\Omega$ ; Stator inductance: 15.86mH;

Rotor resistance: 0.0188 $\Omega$ ; Rotor inductance: 16.2mH; Mutual inductance: 15.66mH;

Generator inertia: 75 kg m<sup>2</sup>; Turbine inertia: 4,052,442 kg m<sup>2</sup>; Shaft stiffness: 83,000,000 Nm/rad.

